

Electronic Supplementary Information (ESI)

A Low-Volume Flow Electrochemical Microreactor for Rapid and Automated Process Optimization

Eduardo Rial-Rodríguez,^{a,b} Johannes F. Wagner,^{a,b} Hans-Michael Eggenweiler,^c
Thomas Fuchss,^c Alena Sommer,^c C. Oliver Kappe,^{a,b} Jason D. Williams^{*,a,b}
and David Cantillo^{*,a,b}

^a *Institute of Chemistry, University of Graz, NAWI Graz, Heinrichstrasse 28, 8010 Graz, Austria.
E-mail: david.cantillo@uni-graz.at*

^b *Center for Continuous Flow Synthesis and Processing (CCFLOW), Research Center
Pharmaceutical Engineering GmbH (RCPE), Inffeldgasse 13, 8010 Graz, Austria. E-mail:
jason.williams@rcpe.at*

^c *Medicinal Chemistry and Drug Design, Merck Healthcare KGaA, Frankfurter Strasse 250,
64293 Darmstadt, Germany*

Table of Contents

S1. Materials and assembly of the microreactor.....	3
S2. Instructions for assembly of the flow microreactor.....	4
S3. Technical drawings of the microreactor and channel layers	5
S4. Experimental setup and general procedures.....	7
S5. Workflow of the automated platform.....	9
S6. Reaction conditions and results of the automated runs.....	10
S7. Statistical analysis of reaction results.....	14
S7.1 <i>tert</i> -Butyltoluene oxidation	14
S7.2 Alcohol oxidation	17
S7.3 Hofer-Moest reaction.....	20
S8. Synthesis and characterization of 6	23
S9. References	25

S1. Materials and assembly of the microreactor

All commercially available chemicals were used as received from Sigma Aldrich, Fisher Scientific, Alfa Aesar, and TCI.

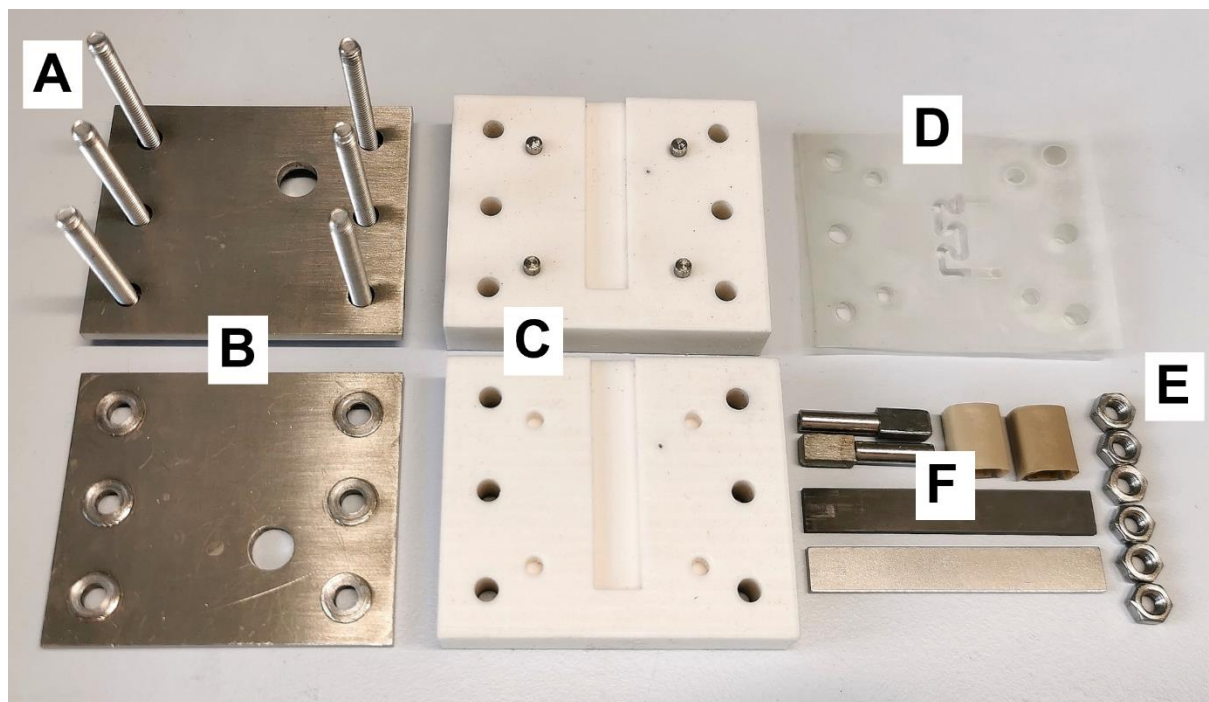


Figure S1. Components of the new flow electrochemical microreactor used.

A: M4 x 35mm full thread hexagon bolts (DIN 933) - Stainless steel (A2)

B: Steel end plates, both identical*

C: PTFE halves of the main body of the cell, both identical*

D: In-house laser cut channel layers, Mylar 0.1 mm thick

E: RS PRO hexagon nuts, M4 stainless steel 7mm smooth A2 304 DIN 934

F: IKA electrodes and the metal pieces used for connecting to the power supply

*Manufactured by Hubs (<https://www.hubs.com/>)

S2. Instructions for assembly of the flow microreactor

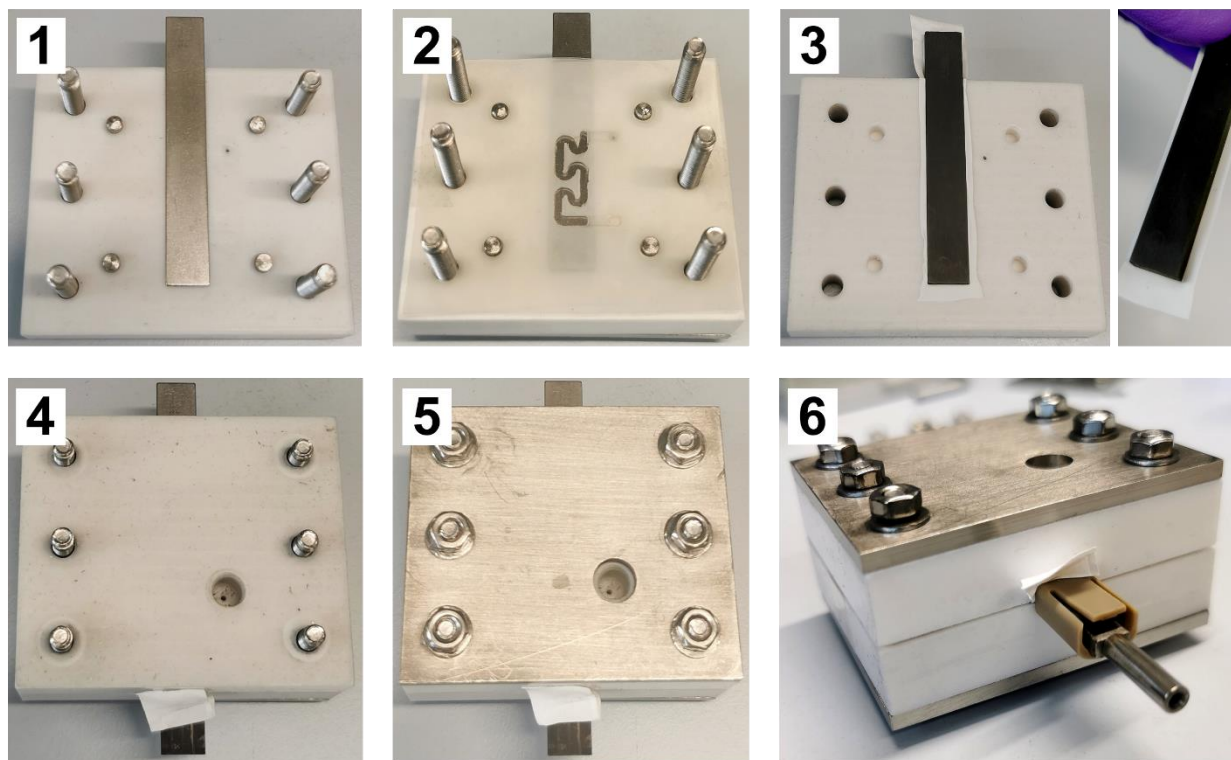


Figure S2. Instructions for the assembly of the flow microreactor

- 1:** On top of a steel end plate, one half of the cell is placed. Then, the IKA electrode is placed in the cavity and six screws are inserted through the holes of both layers. Four steel pins are inserted in a rectangle shape to align the Mylar layers.
- 2:** The three channel layers are arranged in the correct order, putting the main channel in the middle. The surface area of the channel is 56 mm² and its volume 17 μ L.
- 3:** The other electrode is placed in the cavity of the other half cell. In this picture, an example of how to use a thinner electrode is shown. A layer of PTFE thread sealing tape (12mm \times 12mm \times 0.1 mm 60 g/m² DIN EN 751-3) can be placed under the electrode as indicated, allowing the array to have the adequate thickness.
- 4:** The half shown in picture 3 is placed on top of the other half, allowing the screws to go through their holes.
- 5:** The cell is closed with the last steel end plate, and the screws are delicately tightened with the nuts. The hole on the steel plate is used to connect the fluidic fittings (1/4-28) and is connected with the inlet or outlet of the cell.
- 6:** The electrode metal connections for the power supply are assembled, using the plastic adaptors.

S3. Technical drawings of the microreactor and channel layers

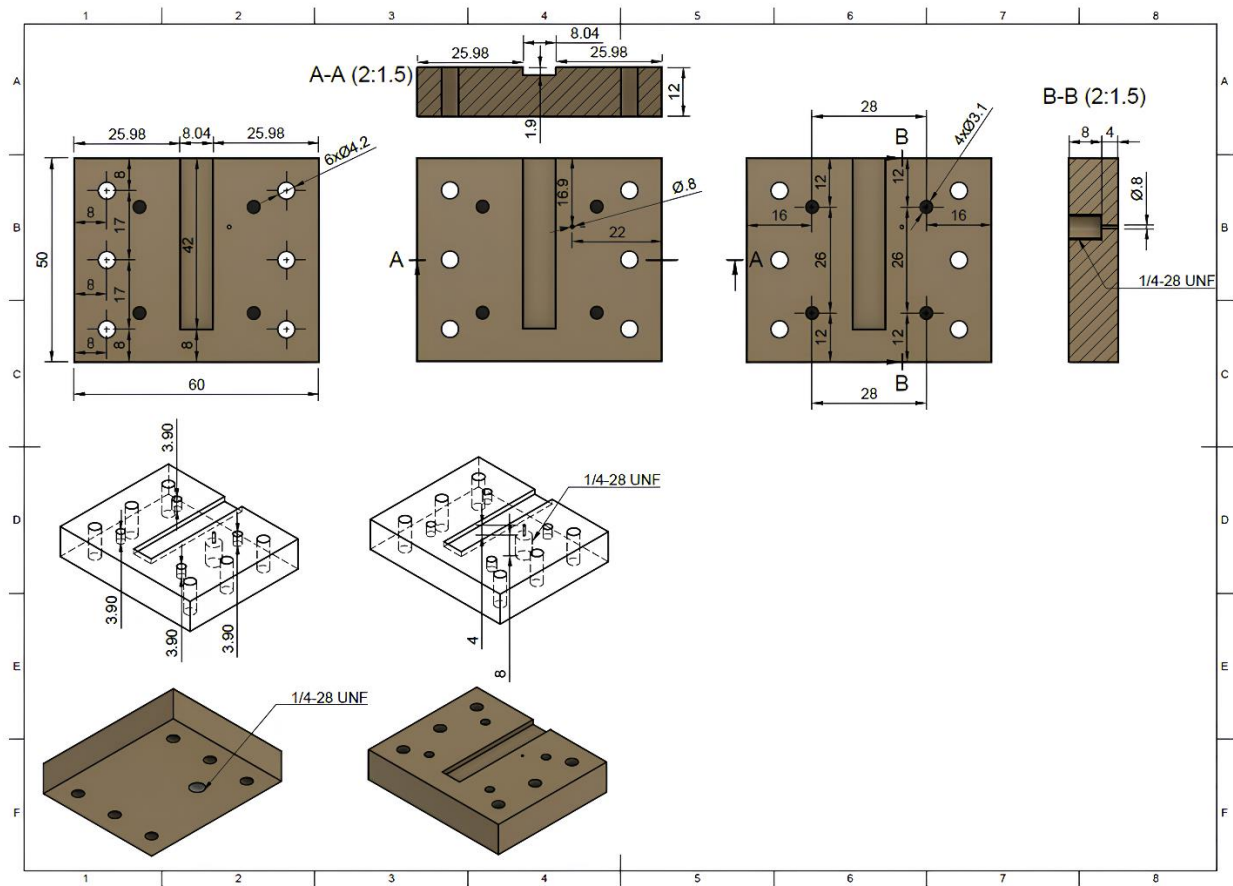


Figure S3. Technical drawing of one half of the cell. All measurements are in mm.

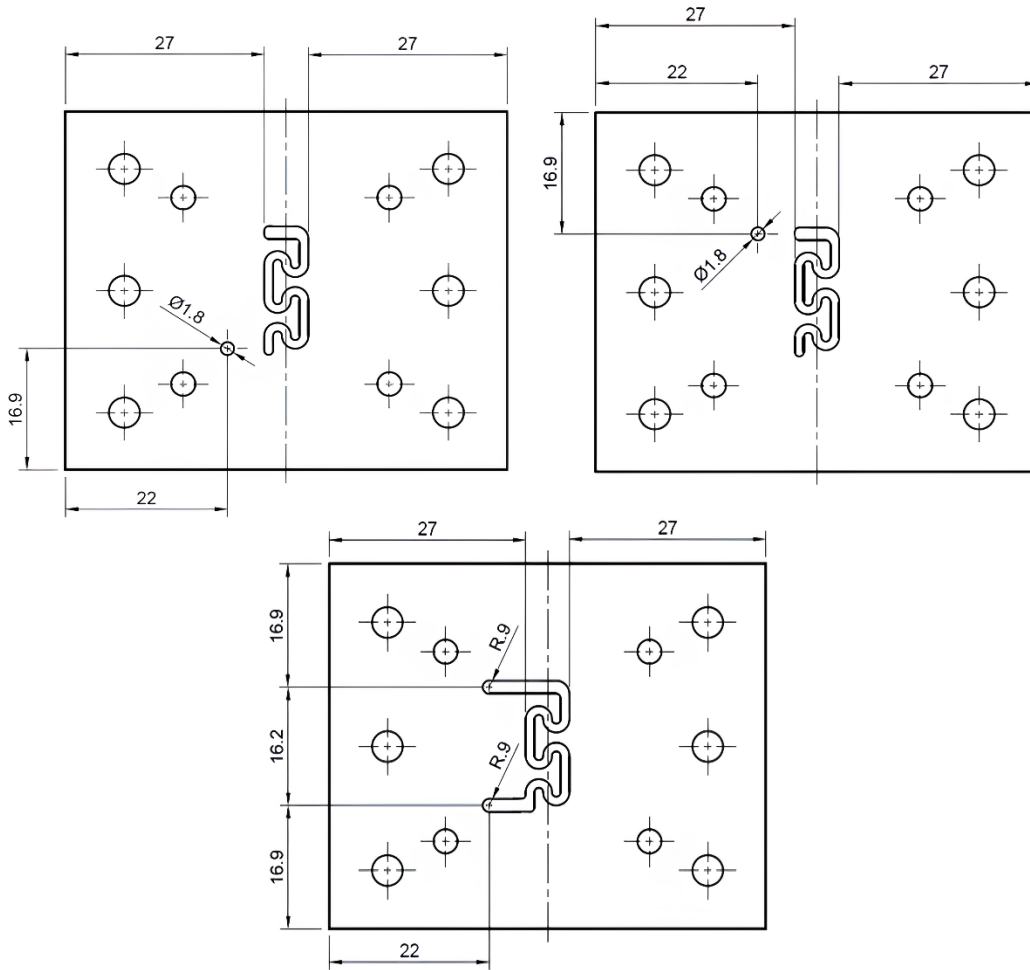


Figure S4. Technical drawing of the channel layers. The bottom drawing represents the main channel that is placed between other two. All numbers are in mm.

S4. Experimental setup and general procedures

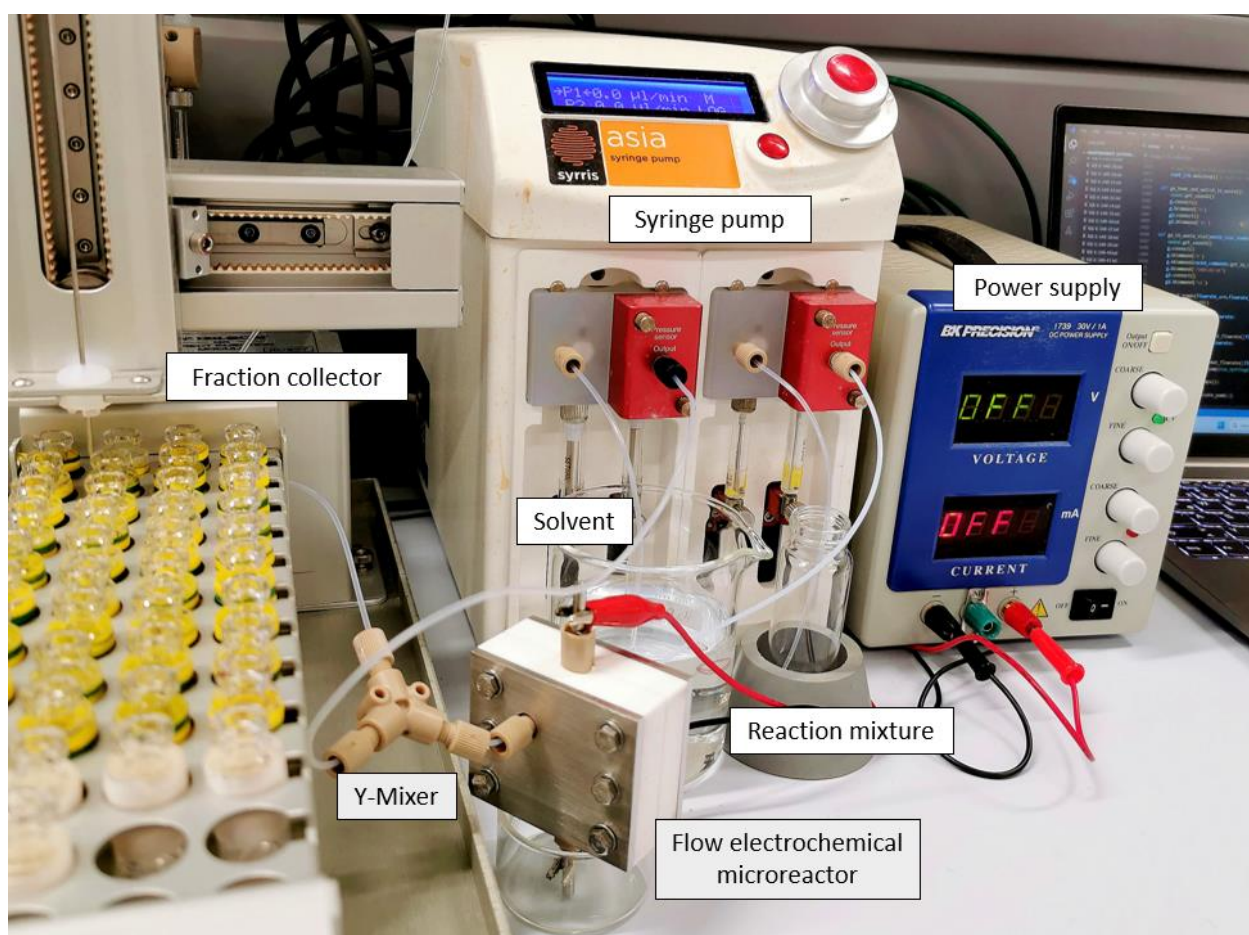


Figure S5. Photograph of the flow electrochemistry platform used for performing the automated runs of experiments with the microreactor.

- **Experimental procedure for the automated screening of electrolysis conditions for the anodic oxidation of 1:** a solution containing **1** (0.1 M) and Et_4NBF_4 (0.1 M) in MeOH was pumped through the flow microreactor using a syringe pump (Syrris, Asia). When the reactor was filled with solution, constant current was applied. At the outlet of the reactor, the reaction mixture was mixed with a MeOH stream at 1.25 mL/min. This diluted mixture was sent to waste until steady-state conditions were reached. The needle was rinsed at the outlet of the fraction collector, then the reactor effluent was collected in an HPLC vial. After the sample was collected, another set of conditions were applied in an automated manner, using the procedure described above.

- **Experimental procedure for the automated screening of electrolysis conditions for the anodic oxidation of 3:** a solution containing **3** (0.025 M), Et₄NBF₄ (0.1 M) and TFA (0.05 M) in MeCN was dried over 3 Å molecular sieves. Then, H₂O (0.05 M) was added and the resulting solution was pumped through the flow microreactor using a syringe pump (Syrris, Asia). When the reactor was filled with solution, constant current was applied. At the outlet of the reactor, the reaction mixture was mixed with an MeCN stream at 0.833 mL/min. This diluted mixture was sent to waste until steady-state conditions were reached. The needle was rinsed at the outlet of the fraction collector, then the reactor effluent was collected in an HPLC vial.
After the sample was collected, another set of conditions were applied in an automated manner, using the procedure described above.
- **Experimental procedure for the automated screening of electrolysis conditions for the anodic oxidation of 5:** a solution containing **5** (0.1 M) and NaOMe (0.1 M) in MeOH was pumped through the flow microreactor using a syringe pump (Syrris, Asia). When the reactor was filled with solution, constant current was applied. At the outlet of the reactor, the reaction mixture was mixed with a MeOH stream at 2.50 mL/min. This diluted mixture was sent to waste until steady-state conditions were reached. The needle was rinsed at the outlet of the fraction collector, then the reactor effluent was collected in an HPLC vial.
After the sample was collected, another set of conditions were applied in an automated manner, using the procedure described above.

S5. Workflow of the automated platform

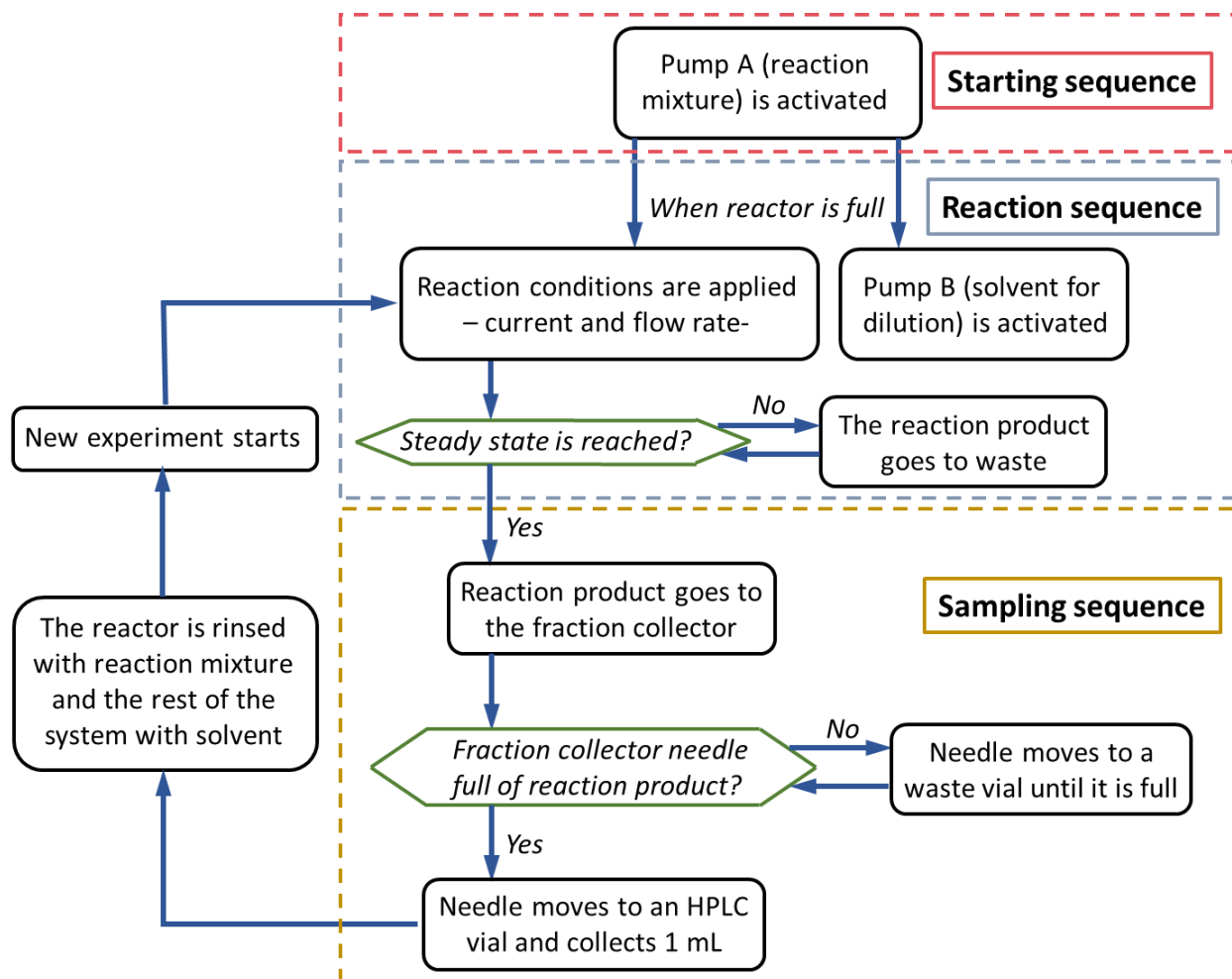


Figure S6. Schematic representation of the workflow of the Python script that controls the automated platform. In order to carry out the experiments, the computer communicates with the pump (via USB), the power supply (via RS-232) and the fraction collector (via RS-232) simultaneously.

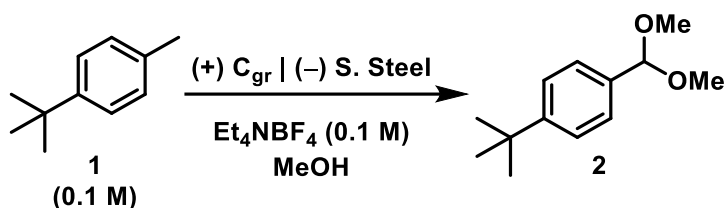
S6. Reaction conditions and results of the automated runs

The yields shown below are based on HPLC area%.

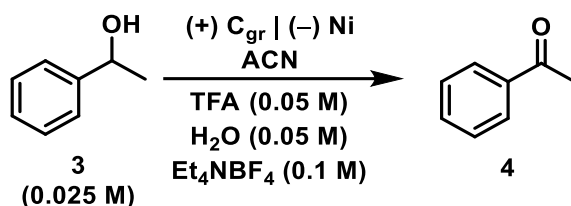
The productivity was calculated using the following expression:

$$Productivity (mg/h) = C (mol/L) * M_{mass} (mg/mol) * Yield (%) * Flow rate (L/h)$$

Table S1. Reaction conditions and results of the automated run for the oxidation of **1**.

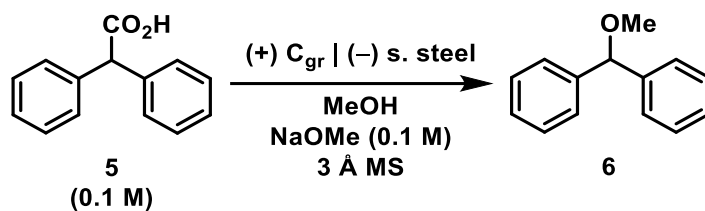


Entry	Current (mA)	Charge (F/mol)	Flow Rate (μL/min)	Yield (%)	Productivity (mg/h)
1	26.0	6.0	26	71.1	23.1
2	26.0	7.0	23	76.1	21.9
3	26.0	8.0	20	78.8	19.7
4	30.0	6.0	31	71.1	27.5
5	30.0	7.0	26	75.8	24.6
6	30.0	8.0	23	78.7	22.6
7	34.0	6.0	35	70.6	30.9
8	34.0	7.0	30	74.2	27.8
9	34.0	8.0	26	75.4	24.5
10	38.0	6.0	39	67.3	32.8
11	38.0	7.0	33	71.5	29.5
12	38.0	8.0	29	73.8	26.8
13	42.0	6.0	43	67.1	36.1
14	42.0	7.0	37	72.5	33.5
15	42.0	8.0	32	74.0	29.6
16	46.0	6.0	47	65.2	38.3
17	46.0	7.0	40	67.2	33.6
18	46.0	8.0	35	71.9	31.5
19	50.0	6.0	51	67.4	43.0
20	50.0	7.0	44	70.3	38.7
21	50.0	8.0	38	71.0	33.7
22	54.0	6.0	55	62.3	42.8
23	54.0	7.0	47	70.5	41.4
24	54.0	8.0	41	70.4	36.1
25	58.0	6.0	60	67.0	50.3
26	58.0	7.0	51	67.3	42.9
27	58.0	8.0	45	68.3	38.4
28	62.0	6.0	64	65.2	52.2
29	62.0	7.0	55	66.7	45.8
30	62.0	8.0	48	57.8	34.7
31	66.0	6.0	68	64.2	54.6
32	66.0	7.0	58	64.7	46.9
33	66.0	8.0	51	62.8	40.0
34	70.0	6.0	72	62.4	56.2
35	70.0	7.0	62	57.0	44.2
36	70.0	8.0	54	53.2	35.9
37	74.0	6.0	76	62.8	59.6
38	74.0	7.0	65	53.8	43.7
39	74.0	8.0	57	53.7	38.3
40	78.0	6.0	80	60.6	60.6
41	78.0	7.0	69	52.4	45.2
42	78.0	8.0	60	52.0	39.0

Table S2. Reaction conditions and results of the automated run for the oxidation of **3**.

Entry	Current (mA)	Charge (F/mol)	Flow Rate (μ L/min)	Yield (%)	Productivity (mg/h)
1	2.5	2.5	24	58.8	2.5
2	2.5	2.8	22	75.8	3.0
3	2.5	3.0	20	85.0	3.1
4	2.7	2.5	26	74.1	3.5
5	2.7	2.8	23	83.7	3.5
6	2.7	3.0	22	88.1	3.5
7	2.9	2.5	28	75.8	3.8
8	2.9	2.8	25	84.4	3.8
9	2.9	3.0	24	86.7	3.7
10	3.1	2.5	30	76.1	4.1
11	3.1	2.8	27	81.6	4.0
12	3.1	3.0	25	86.8	3.9
13	3.3	2.5	32	75.6	4.4
14	3.3	2.8	29	81.8	4.3
15	3.3	3.0	27	84.3	4.1
16	3.5	2.5	34	76.5	4.7
17	3.5	2.8	31	80.9	4.5
18	3.5	3.0	29	83.6	4.4
19	3.7	2.5	36	74.0	4.8
20	3.7	2.8	32	80.8	4.7
21	3.7	3.0	30	81.7	4.4
22	3.9	2.5	38	71.5	4.9
23	3.9	2.8	34	77.4	4.7
24	3.9	3.0	32	79.8	4.6
25	4.2	2.5	41	70.7	5.2
26	4.2	2.8	37	73.5	4.9
27	4.2	3.0	34	78.2	4.8
28	4.5	2.5	44	66.5	5.3
29	4.5	2.8	39	70.8	5.0
30	4.5	3.0	37	71.7	4.8
31	4.8	2.5	47	62.6	5.3
32	4.8	2.8	42	67.1	5.1
33	4.8	3.0	39	70.5	5.0
34	5.2	2.5	51	61.2	5.6
35	5.2	2.8	46	64.1	5.3
36	5.2	3.0	43	64.2	5.0
37	5.6	2.5	55	55.6	5.5
38	5.6	2.8	49	60.1	5.3
39	5.6	3.0	46	55.6	4.6
40	6.0	2.5	59	50.0	5.3
41	6.0	2.8	53	49.8	4.8
42	6.0	3.0	49	50.4	4.4

Table S3. Reaction conditions and results of the automated run done for the Hofer-Moest reaction of 5.



Entry	Current (mA)	Charge (F/mol)	Flow Rate ($\mu\text{L}/\text{min}$)	Yield (%)	Productivity (mg/h)
1	20.0	3.1	40	79.6	37.9
2	20.0	3.2	38	81.2	36.7
3	20.0	3.3	37	82.3	36.2
4	20.0	3.4	36	82.2	35.2
5	20.0	3.5	35	83.4	34.7
6	20.0	3.6	34	82.7	33.4
7	20.0	3.7	33	84.6	33.2
8	30.0	3.1	60	81.6	58.3
9	30.0	3.2	58	82.6	57.0
10	30.0	3.3	56	82.9	55.2
11	30.0	3.4	54	83.6	53.7
12	30.0	3.5	53	83.5	52.6
13	30.0	3.6	51	83.6	50.7
14	30.0	3.7	50	84.8	50.4
15	40.0	3.1	80	81.8	77.9
16	40.0	3.2	77	82.0	75.1
17	40.0	3.3	75	83.7	74.7
18	40.0	3.4	73	83.6	72.6
19	40.0	3.5	71	83.7	70.7
20	40.0	3.6	69	84.9	69.7
21	40.0	3.7	67	85.5	68.2
22	50.0	3.1	100	82.4	98.0
23	50.0	3.2	97	83.1	95.9
24	50.0	3.3	94	83.8	93.7
25	50.0	3.4	91	84.3	91.2
26	50.0	3.5	88	84.9	88.9
27	50.0	3.6	86	85.5	87.4
28	50.0	3.7	84	85.8	85.7
29	60.0	3.1	120	81.0	115.7
30	60.0	3.2	116	82.6	114.0
31	60.0	3.3	113	82.9	111.5
32	60.0	3.4	109	84.0	108.9
33	60.0	3.5	106	84.7	106.8
34	60.0	3.6	103	85.8	105.1
35	60.0	3.7	100	86.3	102.6
36	70.0	3.1	140	79.3	132.1
37	70.0	3.2	136	81.3	131.6
38	70.0	3.3	131	82.3	128.2
39	70.0	3.4	128	82.2	125.2
40	70.0	3.5	124	83.3	122.8
41	70.0	3.6	120	84.4	120.5
42	70.0	3.7	117	84.5	117.6

S7. Statistical analysis of reaction results

All statistical analysis was carried out using Sartorius Modde v13.

S7.1 *tert*-Butyltoluene oxidation

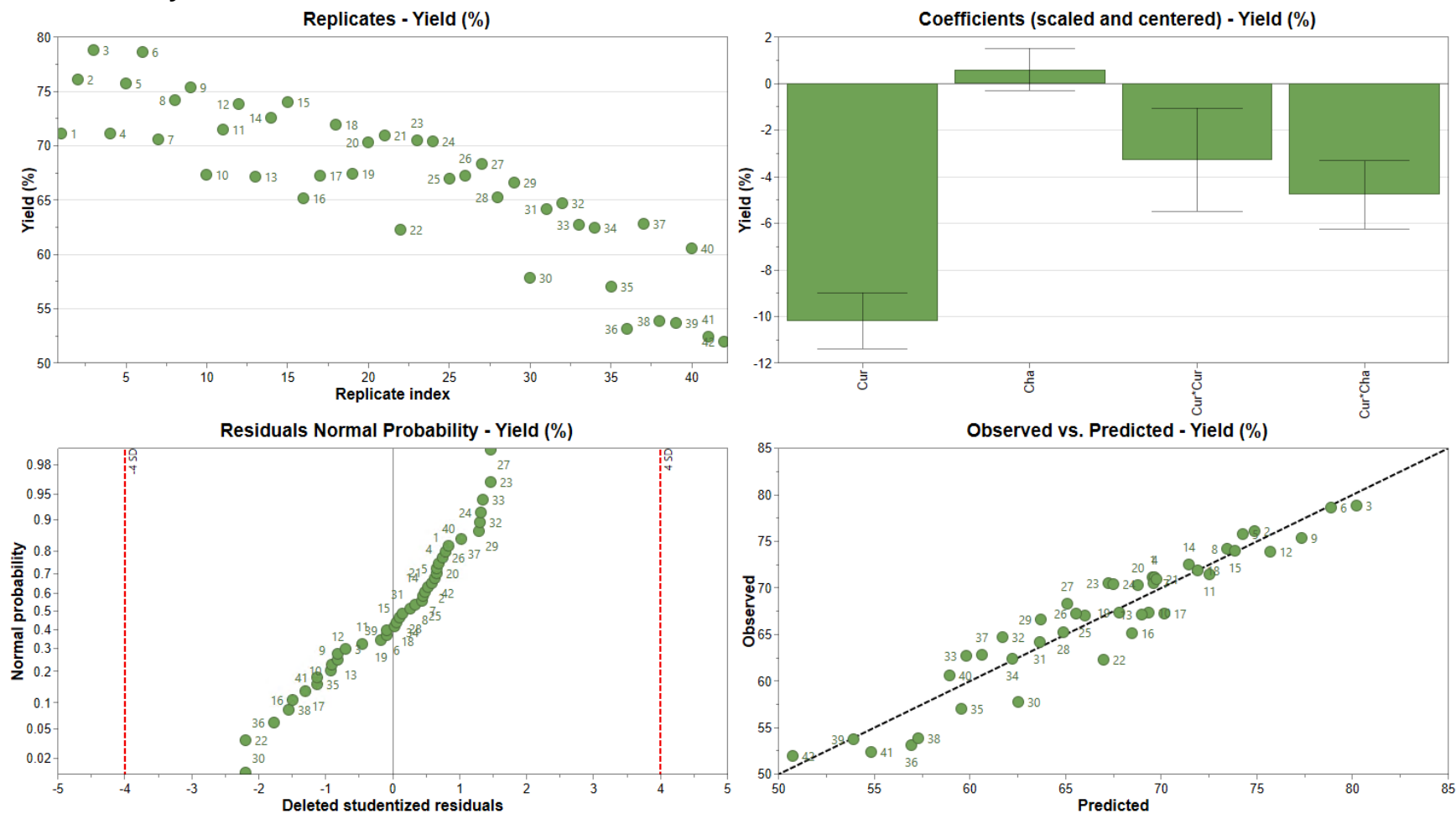


Figure S7. Model summary for the **yield** achieved in oxidation of *tert*-butyltoluene **1**. $R^2 = 0.9035$, $Q^2 = 0.8792$.

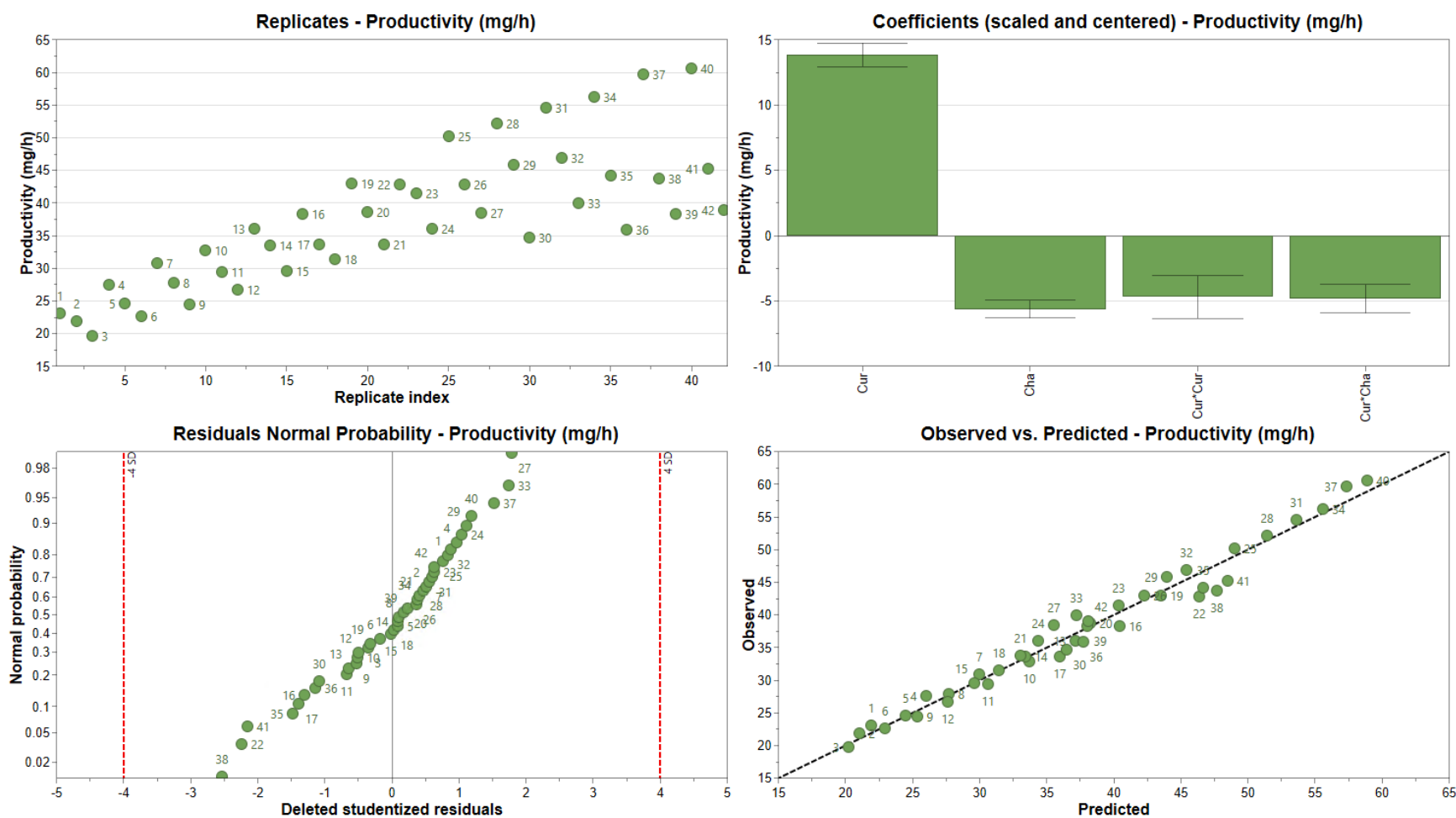


Figure S8. Model summary for the **productivity** achieved in oxidation of *tert*-butyltoluene **1**. $R^2 = 0.97439$, $Q^2 = 0.9671$.

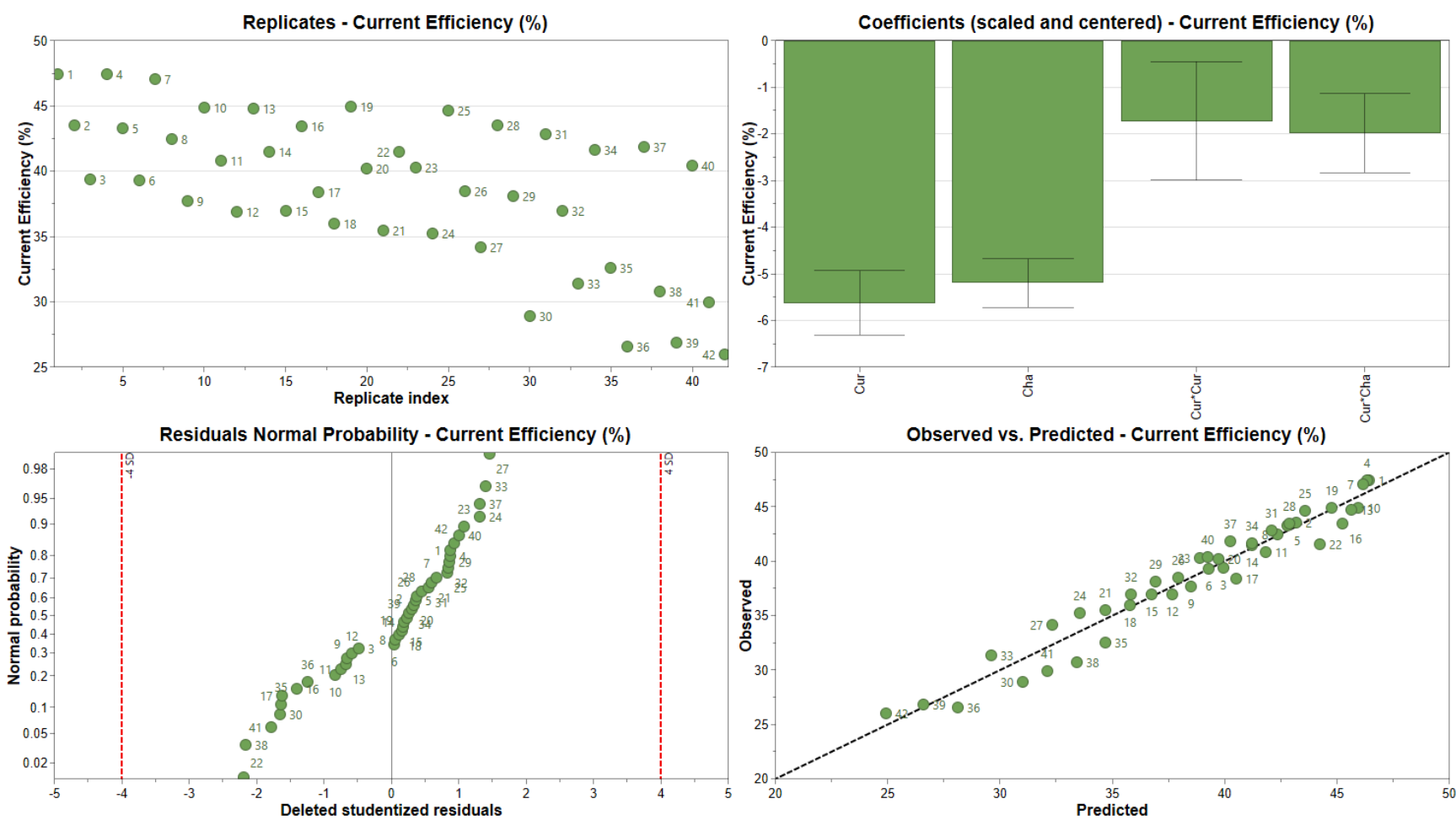


Figure S9. Model summary for the **current efficiency** achieved in oxidation of *tert*-butyltoluene **1**. $R^2 = 0.9505$, $Q^2 = 0.9369$.

S7.2 Alcohol oxidation

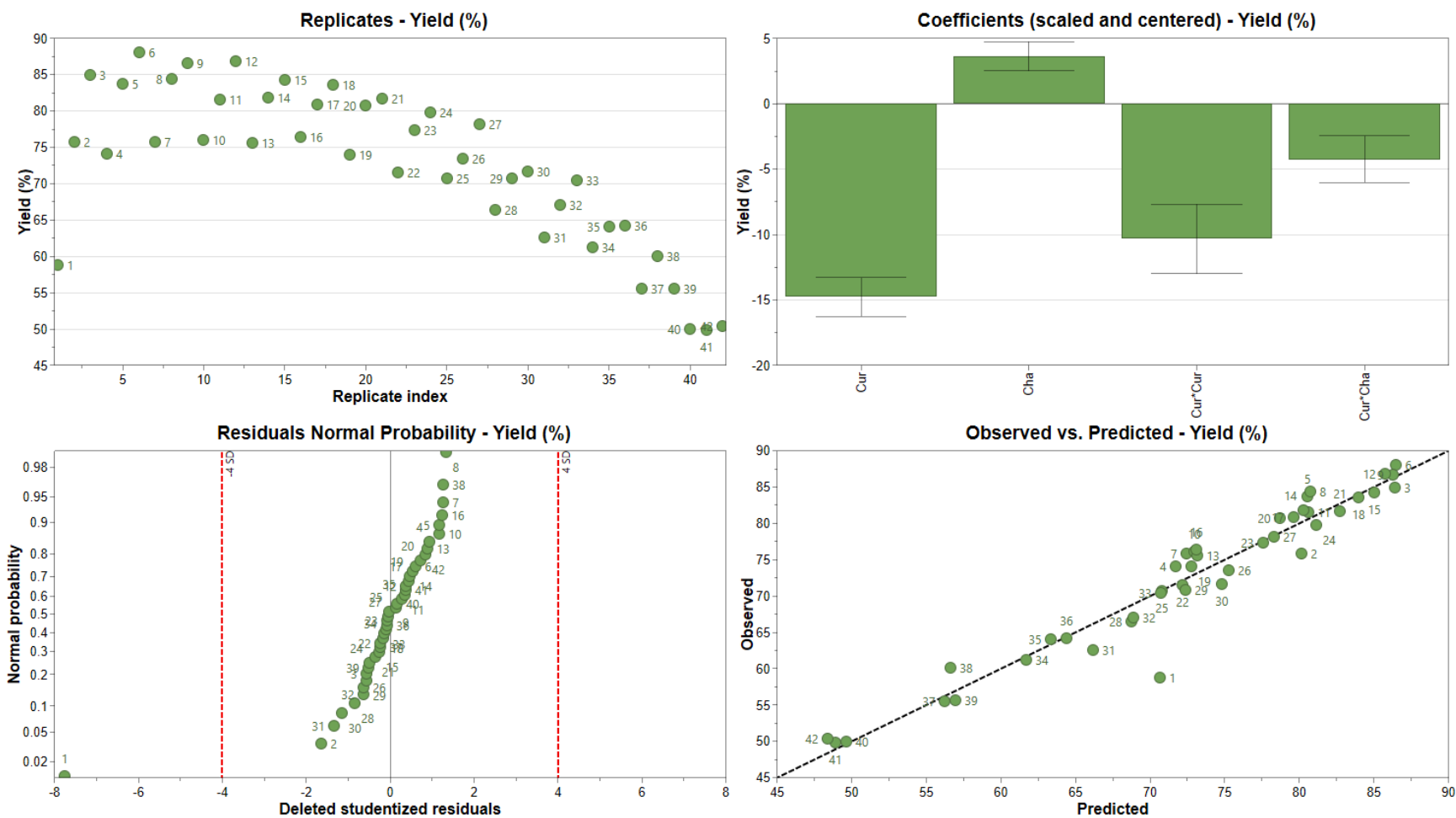


Figure S10. Model summary for the **yield** achieved in oxidation of benzylic alcohol **3**. $R^2 = 0.9361$, $Q^2 = 0.9024$.

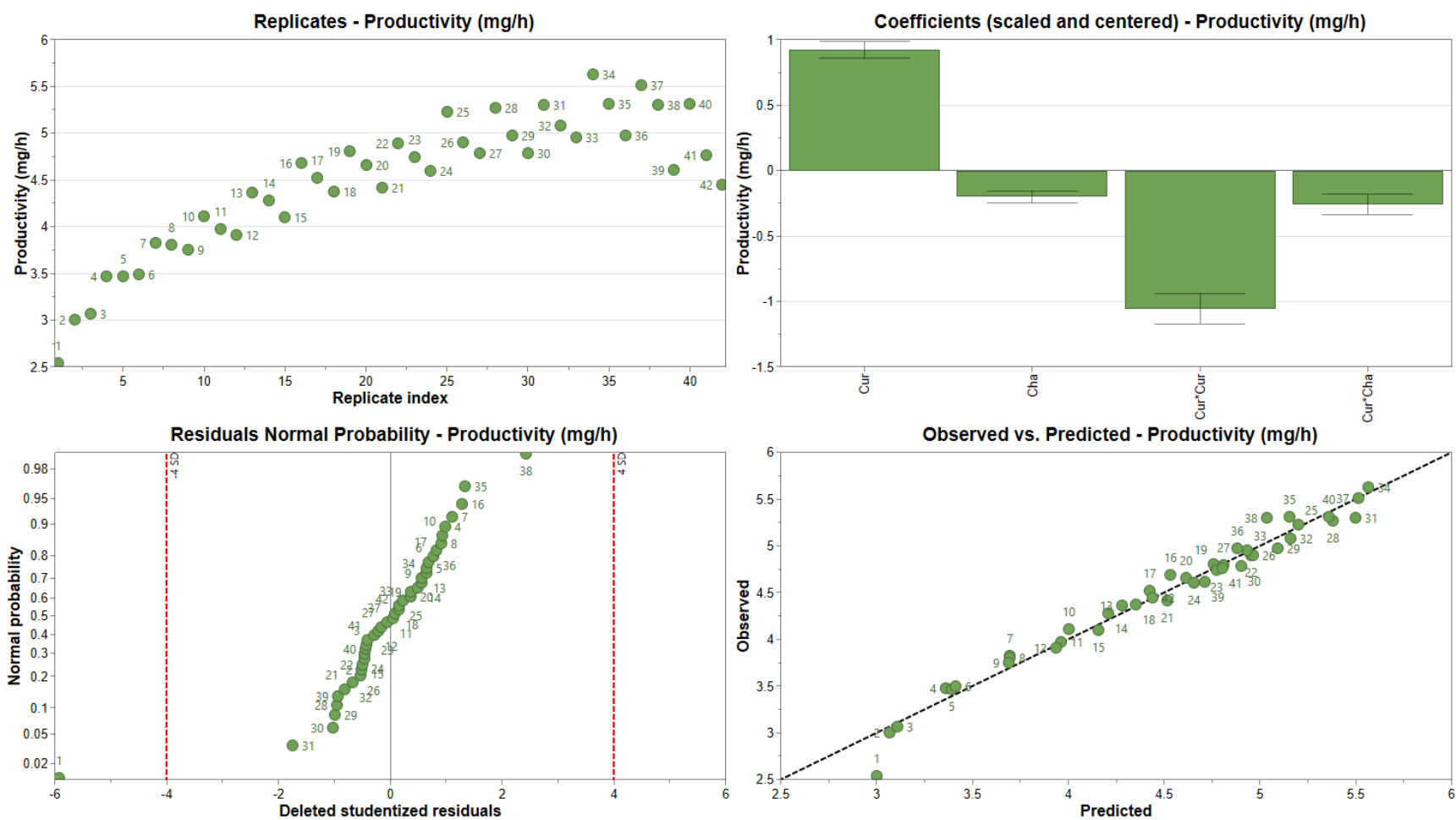


Figure S11. Model summary for the **productivity** achieved in oxidation of benzylic alcohol **3**. $R^2 = 0.9735$, $Q^2 = 0.9614$.

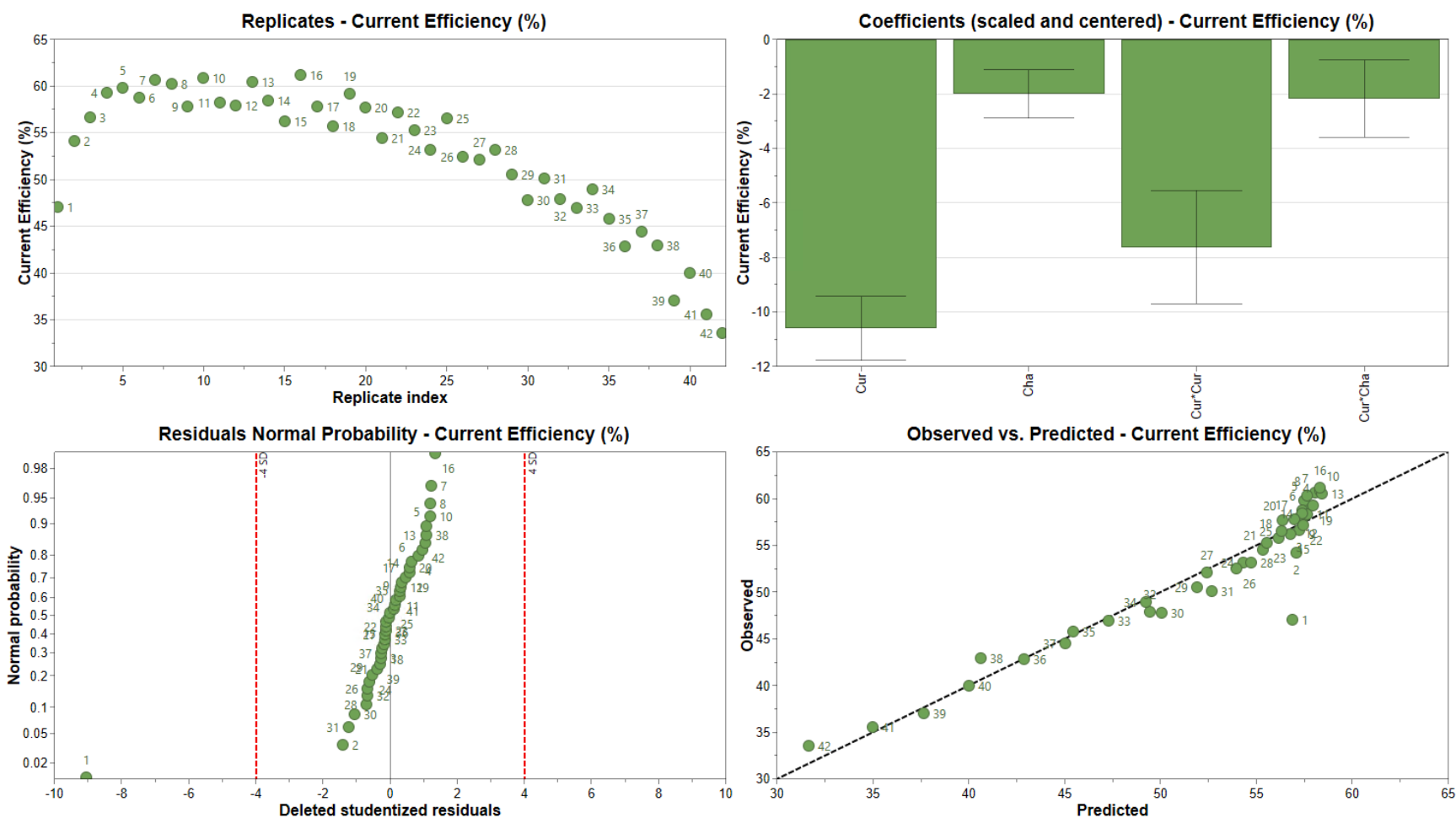


Figure S12. Model summary for the **productivity** achieved in oxidation of benzylic alcohol **3**. $R^2 = 0.9162$, $Q^2 = 0.8694$.

S7.3 Hofer-Moest reaction

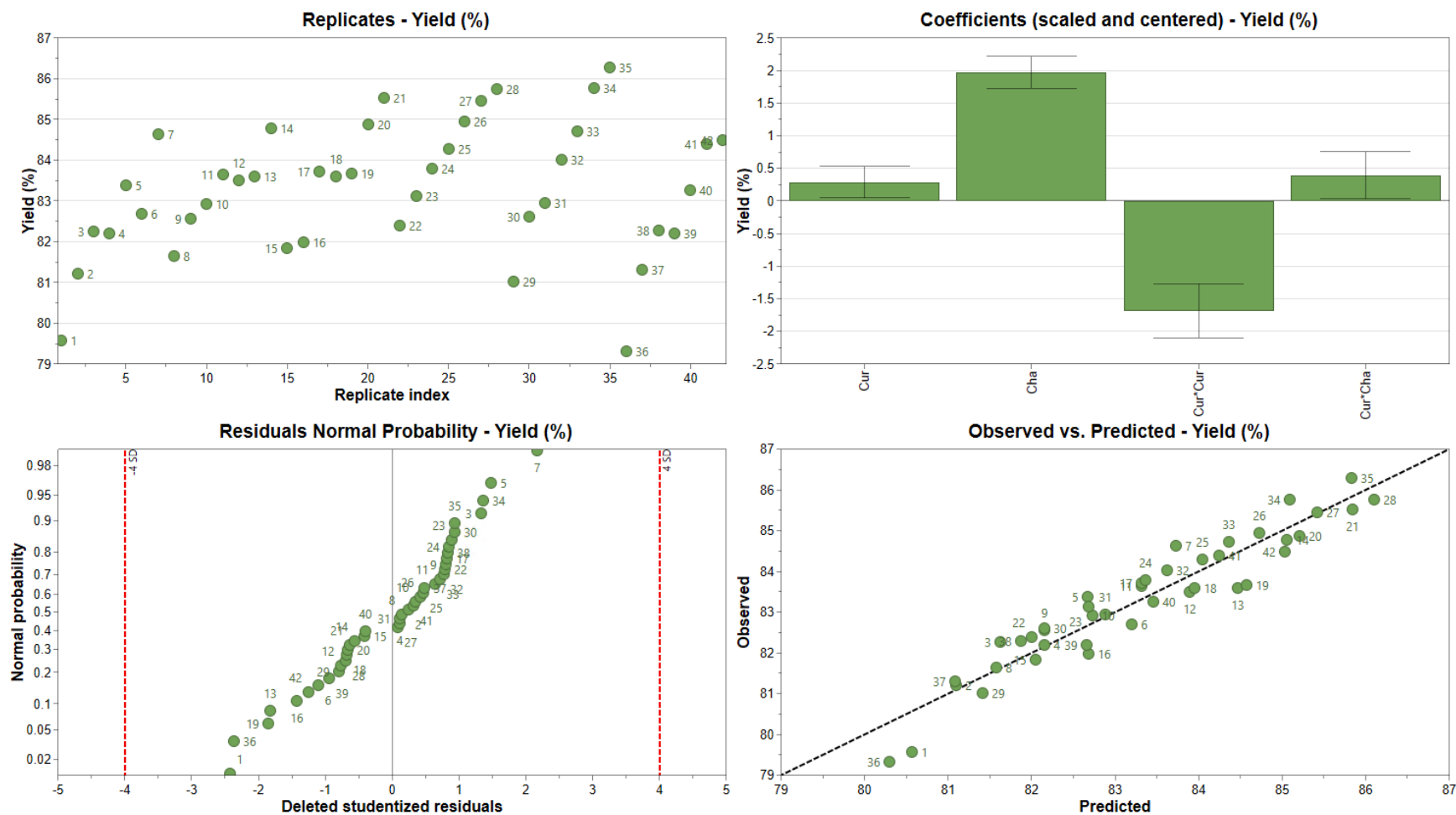


Figure S13. Model summary for the **yield** achieved in the Hofer-Moest reaction of carboxylic acid **3**. $R^2 = 0.9040$, $Q^2 = 0.8602$.

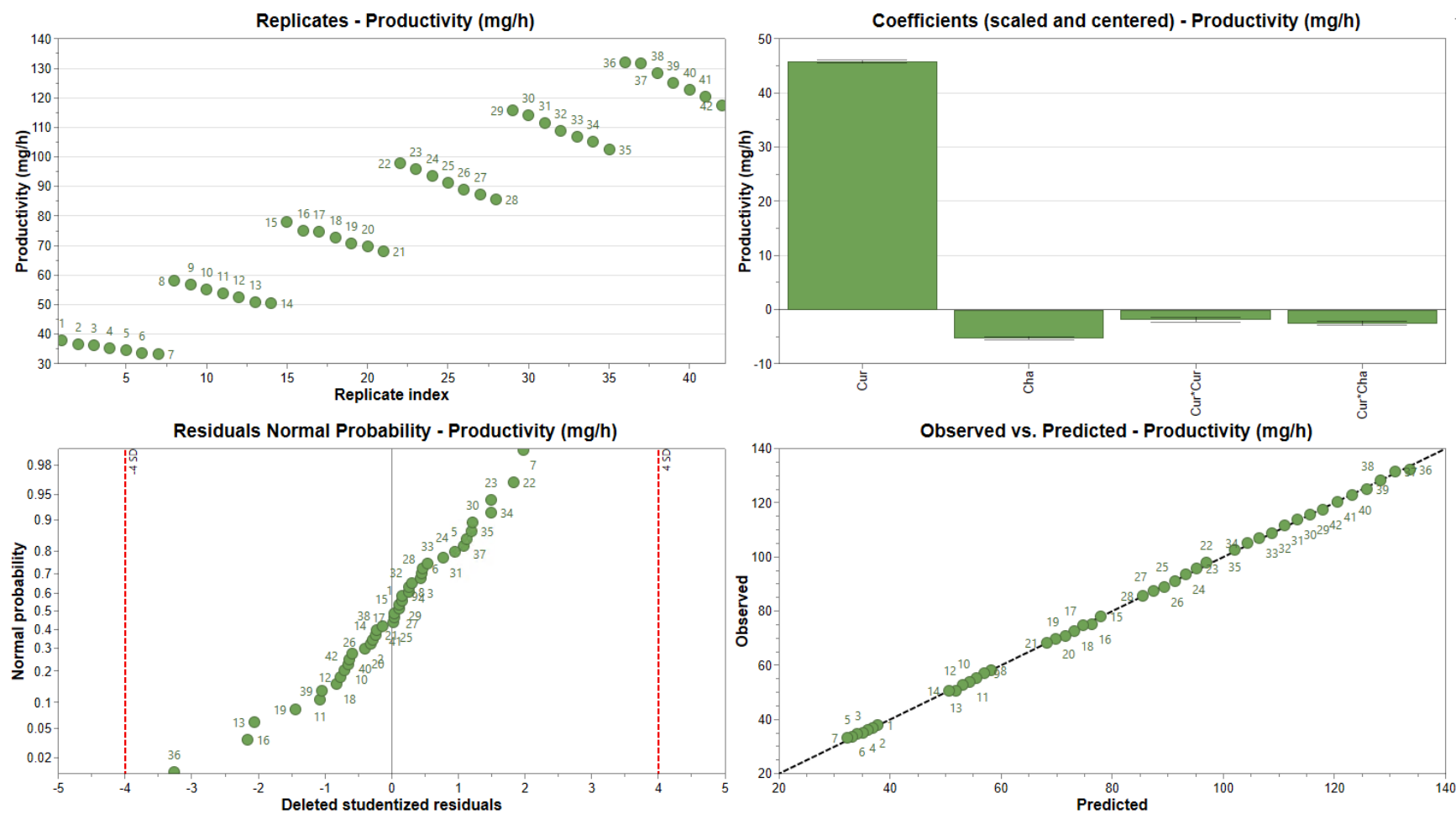


Figure S14. Model summary for the **productivity** achieved in the Hofer-Moest reaction of carboxylic acid **3**. $R^2 = 0.9997$, $Q^2 = 0.9996$.

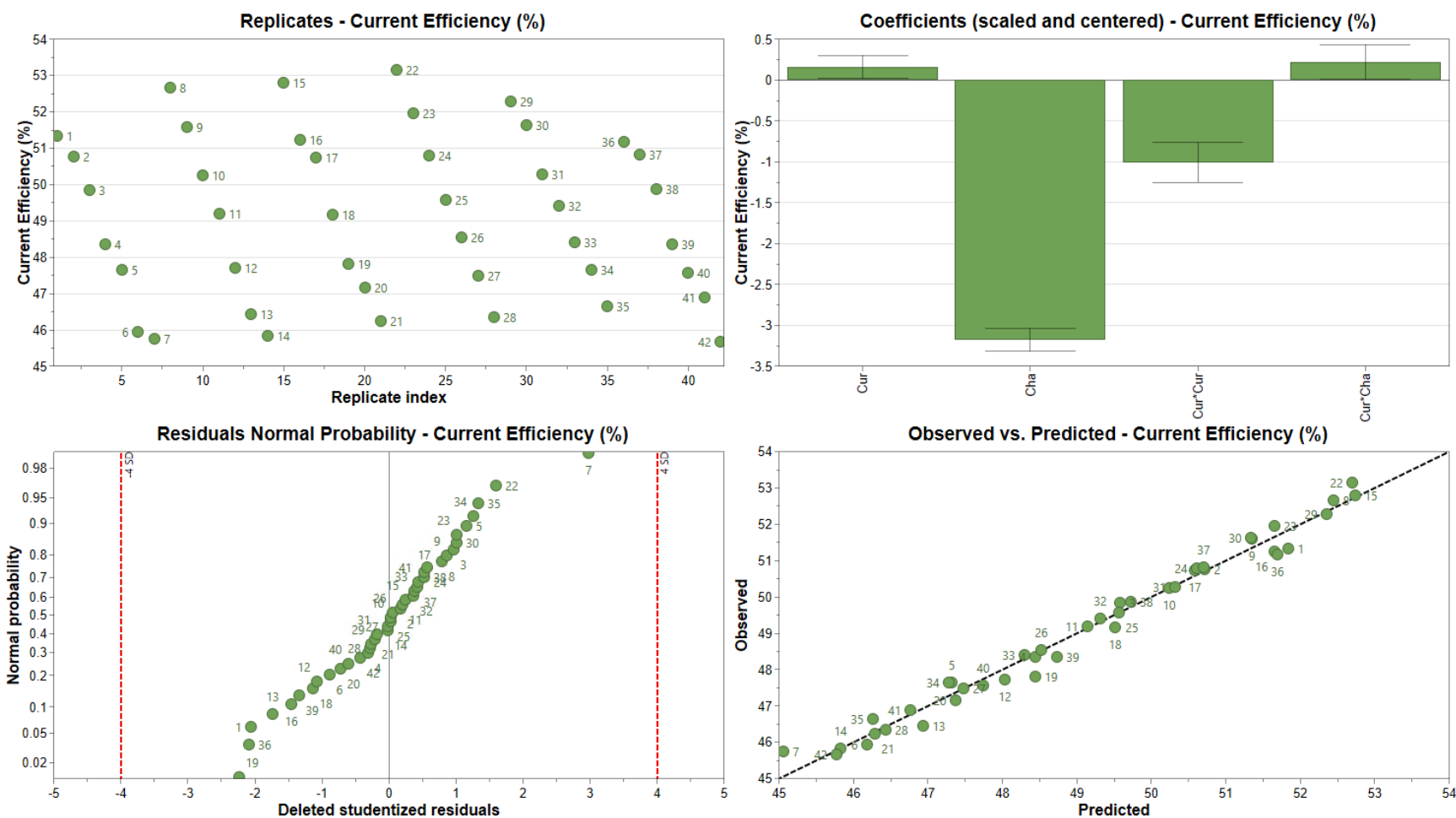
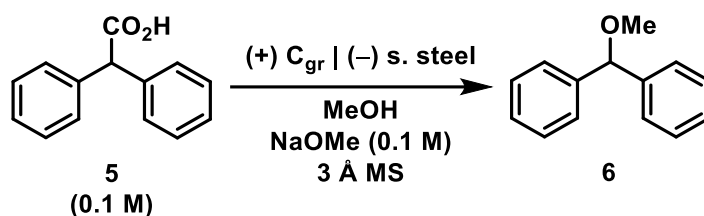


Figure S15. Model summary for the **current efficiency** achieved in the Hofer-Moest reaction of carboxylic acid **3**. $R^2 = 0.9827$, $Q^2 = 0.9750$. Note: a response surface plot based on this model is shown in manuscript **Fig 3D**.

S8. Synthesis and characterization of 6



A 50 mL solution of **5** (1.06 g, 5.0 mmol, 0.1 M) and NaOMe (270 mg, 5.0 mmol, 0.1 M) in MeOH was prepared. The mixture was pumped through the previously-described electrolysis cell¹ at a flow rate of 1.30 mL/min. When the reactor was filled with solution, a constant current of 689 mA was applied (1.08 mA/cm² calculated current density). Once steady-state conditions were reached, the reaction mixture was collected from the output for 31 min. After that, the solvent was evaporated under reduced pressure and the residue was redissolved in dichloromethane. The resulting solution was washed with saturated aqueous NaHCO₃ solution (1 × 20 mL), and the aqueous layer was extracted with dichloromethane (2 × 25 mL). The combined organic layers were washed with water (1 × 20 mL), brine (1 × 25 mL), dried over Na₂SO₄ anhydrous, filtered and evaporated under reduced pressure to yield **6** (727 mg, 85% yield) as a yellow oil. Characterization of the product matched previous literature reports.¹

¹H NMR (300 MHz, DMSO-*d*₆) δ 7.39 – 7.21 (m, 10H), 5.33 (s, 1H), 3.27 (s, 3H).

¹³C NMR (75 MHz, DMSO-*d*₆) δ 142.9, 128.8, 127.7, 126.9, 84.6, 56.8.

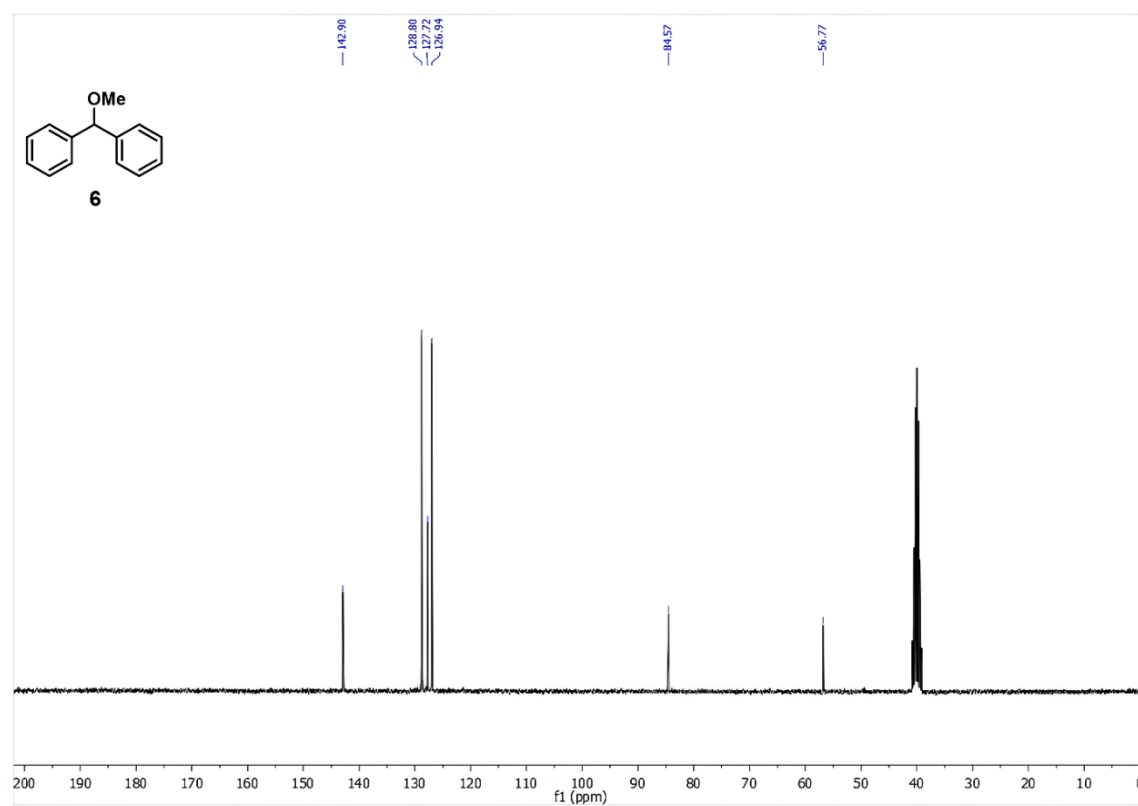
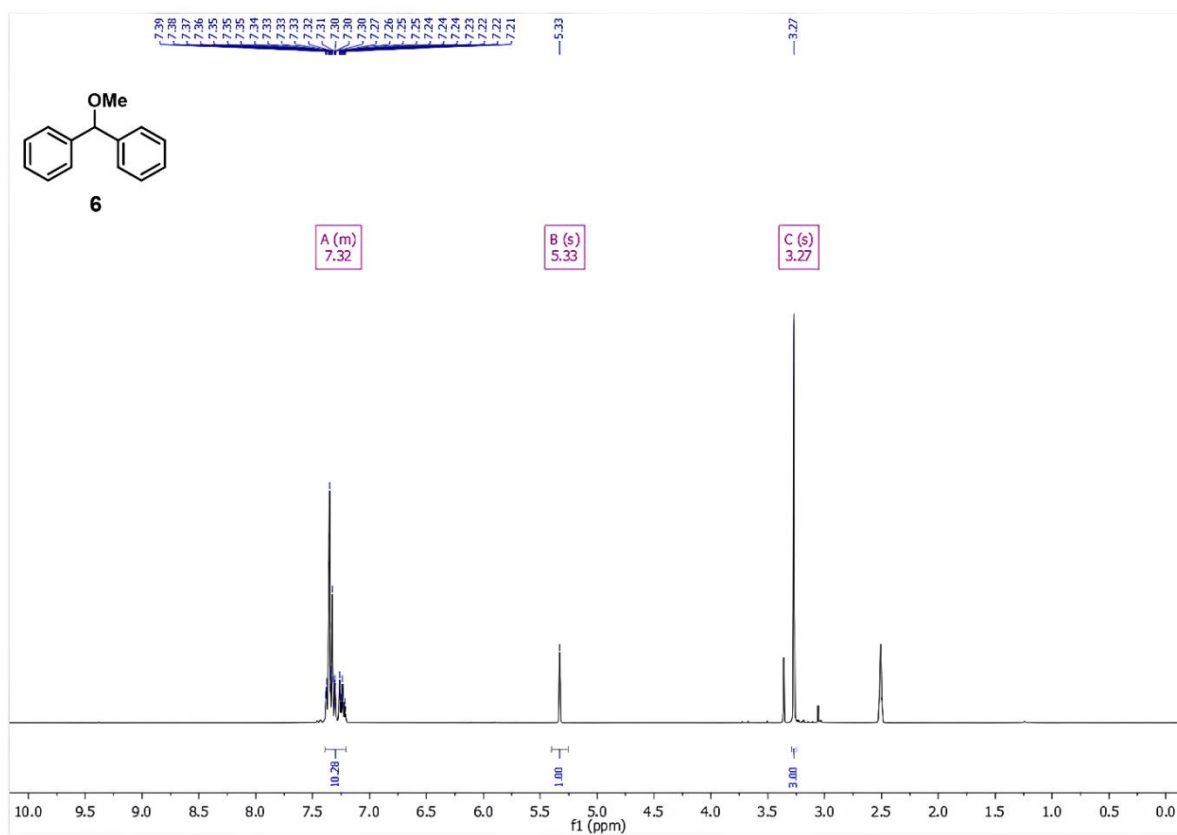


Figure S16. ¹H NMR (top) and ¹³C NMR (bottom) of the isolated product **6**.

S9. References

¹W. Jud, C. O. Kappe and D. Cantillo, *Chemistry–Methods*, 2021, **1**, 36–41.